Relativistic Nonthermal Particle Acceleration in Magnetic Reconnection…

and other select topics

Dmitri Uzdensky

(University of Colorado Boulder)

With Univ. Colorado Theoretical Plasma Astrophysics Group:

- Greg Werner
- Vladimir Zhdankin
- Mitch Begelman

(support by NSF, NASA, DOE)

11th WPI Plasma Kinetics Workshop, July 26, 2018

OUTLINE

1. PIC sims of Kinetic Turbulence in Semi-Relativistic *e-ion* Plasmas:

Key point: Electron/Ion Energy Partition: $Q_e/Q_i \sim (\rho_e/\rho_i)^{2/3}$

2. Relativistic Turbulence with Strong Synchrotron (and synchrotron self-Compton, SSC) Radiative Cooling:

Key point: *Thermal balance between turbulent heating and synchrotron cooling (both $\sim B^2/8\pi$) --- yields saturation temperature:*

$\boldsymbol{\vartheta = T/m_e c^2 \sim \tau_T^{-1/2}}$ *(where $\tau_T = n_e L \sigma_T << 1$).*

3. Relativistic Nonthermal Particle Acceleration (NTPA) in Plasmoid-Mediated Magnetic Reconnection:

Key points: *(a) Power-law slope controlled by balance between acceleration by E_{rec} and magnetization by reconnected magnetic field;*

(b) Cutoff is due trapping in plasmoids and controlled by plasmoid distribution function.

1. Driven Kinetic Turbulence in Collisionless Semi-relativistic Electron-Ion Plasmas

V. Zhdankin, G. Werner, D. Uzdensky, M. Begelman (2018, in prep.)

- 3D PIC (Zeltron) simulations of driven kinetic turbulence in collisionless magnetized electron-ion ($m_i = m_p = 1836\ m_e$) plasma.
- 3D Periodic box, $L_x = L_y = L_z$
- Initially: uniform relativistic Maxwellian e-i plasma with $T_{e0} = T_{i0} = T_0$;
- ***Semi-relativistic*** plasma: $m_e c^2 \ll T_0 < m_i c^2$ (ultra-rel. e-s, non-rel. ions)
- Uniform background magnetic field B_0;
- Turbulence driven at large scales by volumetric EM driving (Langevin antenna, TenBarge et al. 2014); with amplitude such that $B_{rms} = B_0$.
- Two main dimensionless parameters:
  - $\theta_{i0} = T_0/m_i c^2 = (1/2048\ \text{--}\ 10)$
  - $\beta_0 = 0.1 - 20$ (most runs are for $\beta_0 = 4/3$)
- Typical system sizes ($512^3 - 768^3$): $L = 256\text{-}384\ \rho_{e0}$ ($\rho_{e0} = 2\ \Delta x$)
- Largest run (1024^3): $L = 512\ \rho_{e0}$, $\beta_0 = 4/3$ and $\theta_{i0} = 1/256$

1. Driven Kinetic Turbulence in Collisionless Semi-relativistic Electron-Ion Plasmas

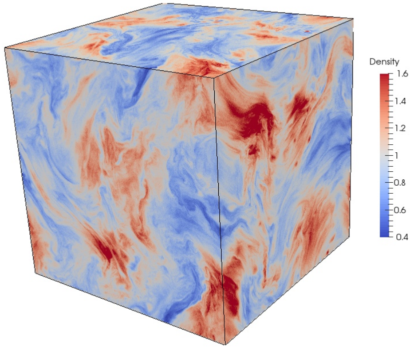

Electron-Ion Energy Partition:

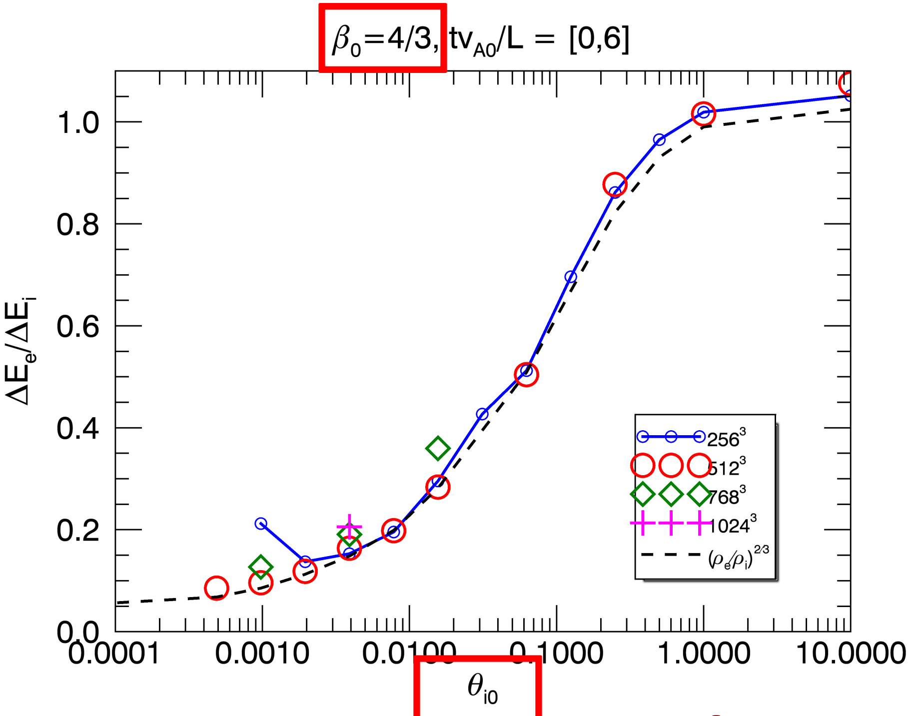

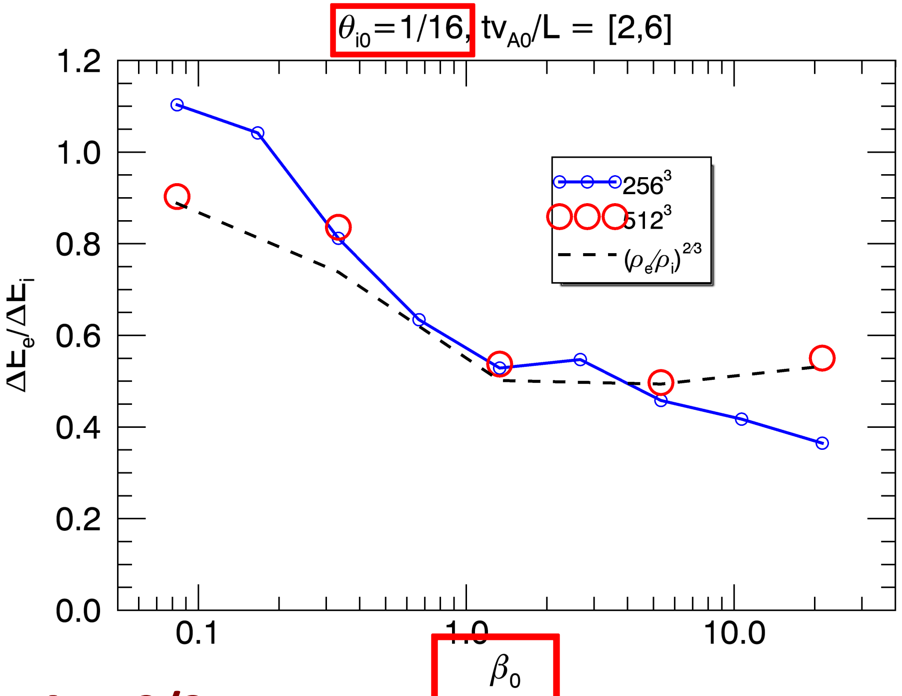

$$Q_e/Q_i \approx (\rho_e/\rho_i)^{2/3}$$

1. Driven Kinetic Turbulence in Collisionless Semi-relativistic Electron-Ion Plasmas

Other Results:

Turbulent Magnetic Spectrum

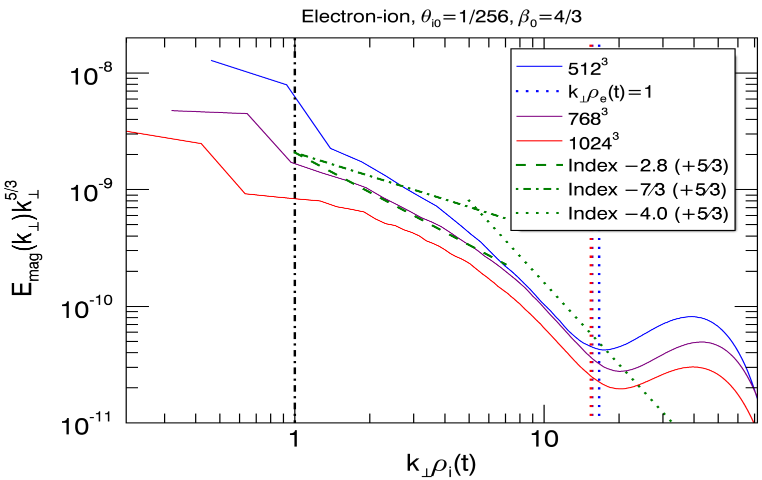

Particle energy spectra

(solid: electrons, dashed: ions)

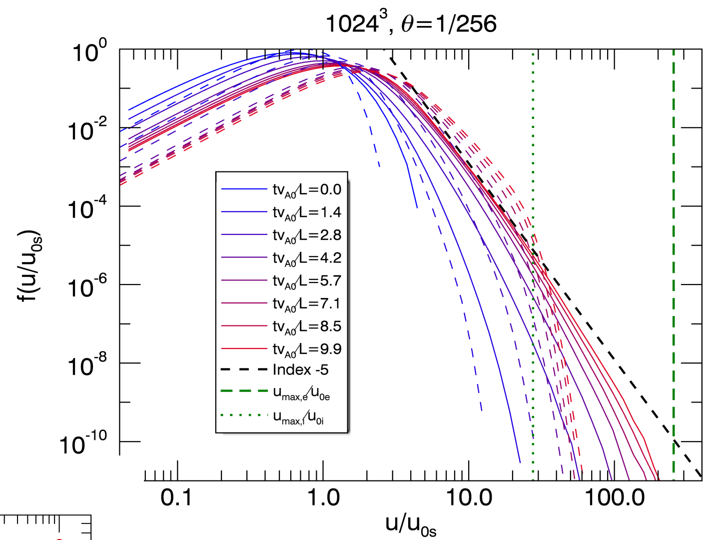

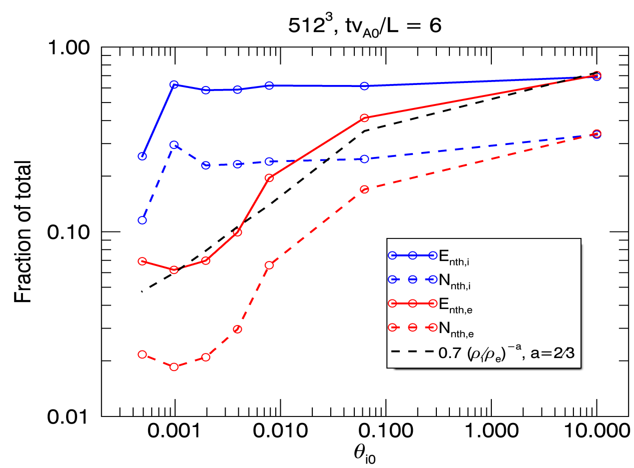

Blue: ions

Red: electrons

SUMMARY 1

- 3D PIC simulations of kinetic plasma turbulence in relativistic plasmas.
- Electron/Ion heating ratio in driven collisionless relativistic or semi-relativistic electron-ion plasmas:

$$Q_e/Q_i \approx (\rho_e/\rho_i)^{2/3}$$


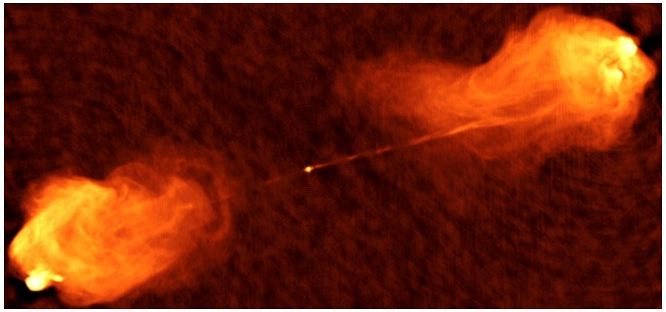


Relativistic MHD Turbulence with Synchrotron and SSC Cooling

(D. Uzdensky, MNRAS 2018)

11th WPI Plasma Kinetics Workshop, Vienna, July 26, 2018

Driven Relativistic MHD Turbulence with Synchrotron Cooling

- Consider relativistic MHD turbulence, driven at scale L, in optically-thin relativistically-hot plasma of density n_e.
- Balance between turbulent heating and radiative cooling:
- Turb. MHD heating rate: $Q_{\text{heat}} \sim (B^2/8\pi) v_{\text{turb}}/L \sim (B^2/8\pi)\, c/L$
- Opt.-thin synchrotron cooling rate: $Q_{\text{sync}} \sim n_e c\, \sigma_T\, (B^2/8\pi)\, \overline{\gamma^2}$
- Heating/Cooling balance: $Q_{\text{heat}} \sim Q_{\text{sync}}$

$$\cancel{(B^2/8\pi)}\ \cancel{c}/L \sim n_e\, \cancel{c}\, \sigma_T\, \cancel{(B^2/8\pi)}\, \gamma^2$$

$$\Rightarrow \quad \gamma^2 \sim 1/\tau_T, \qquad \tau_T = n_e L \sigma_T << 1$$

$$\boldsymbol{\vartheta = T/m_e c^2 \sim 1/\sqrt{\tau_T}}$$

– **universal scaling, independent of $\boldsymbol{B}$!**

Synchrotron-Self-Compton (SSC) Cooling and Compton Catastrophe

- SSC (inverse-Compton scattering of synchrotron photons):

  $Q_{ssc} \sim n_e\, c\, \sigma_T\, U_{\mathrm{rad,\,synch}}\, \gamma^2$ $\qquad$ $Q_{sync} \sim n_e\, c\, \sigma_T\, (B^2/8\,\pi)\, \gamma^2$

- Thus, $Q_{ssc} \sim Q_{sync}\, (U_{\mathrm{rad,\,synch}}/U_{mag})$ $\qquad$ $(U_{mag} = B^2/8\,\pi)$

- Synchrotron radiation energy density:

$$U_{\mathrm{rad,sync}} \sim Q_{sync}\, L/c \sim Q_{heat}\, L/c \sim (B^2/8\,\pi)\, (\mathrm{c}/\cancel{\mathrm{L}})\, \mathrm{L}/\cancel{\mathrm{c}} \sim B^2/8\,\pi = U_{mag}$$

- Thus, $Q_{SSC} \sim Q_{sync}$ – SSC power is comparable to synchrotron!

- Similar arguments for higher-order inverse-Compton (IC scattering of SSC photons, etc.,) → discrete sequence of IC components, separated by $\gamma^2 \sim 1/\tau_T$ in photon energy, slowly declining in power (analogous to IC cooling catastrophe).]

Sketch of Broadband Spectrum

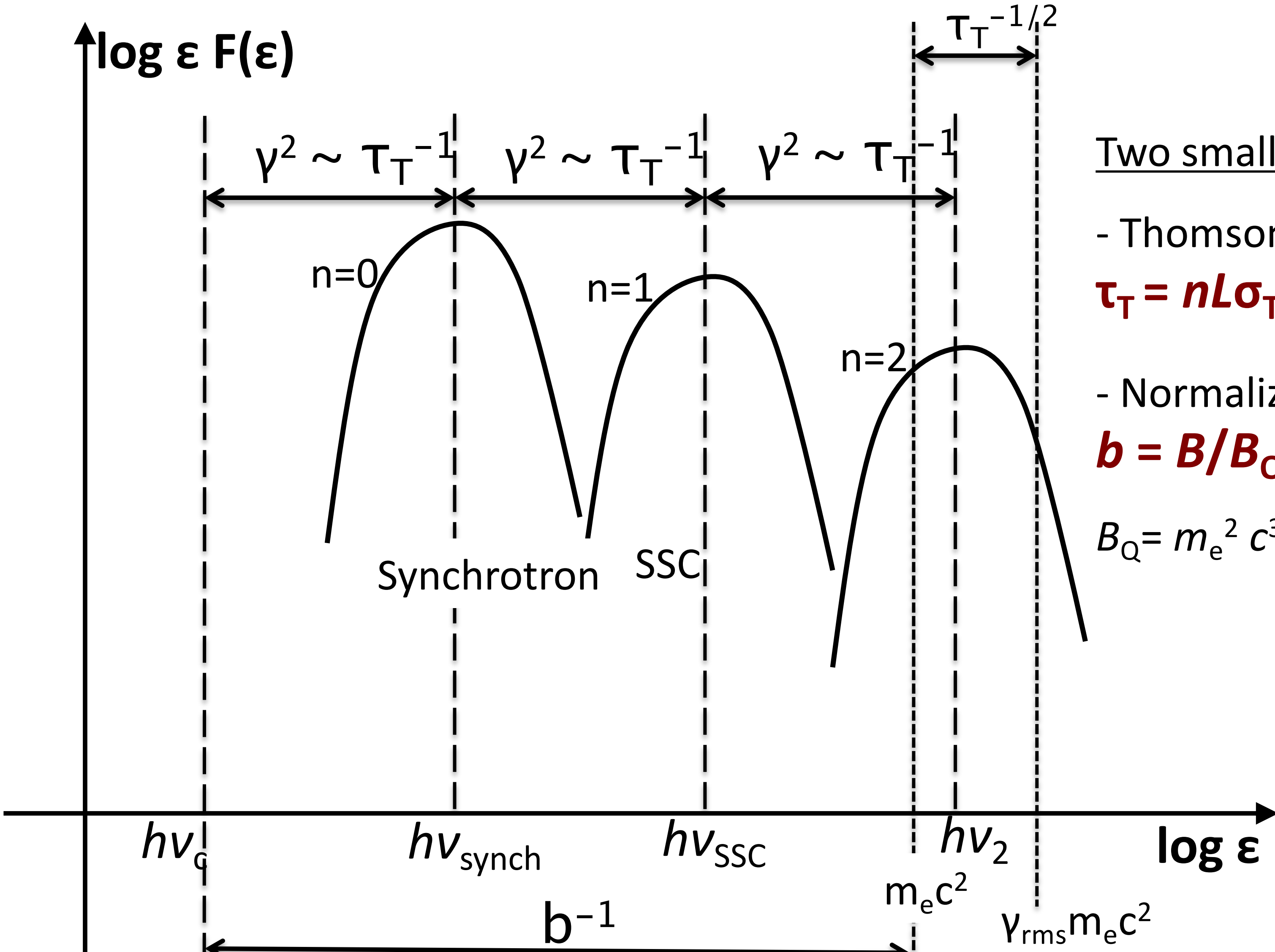

$\overline{\gamma^2} \sim 1/\tau_T$

Two small parameters:

- Thomson optical depth:

$\boldsymbol{\tau_T = nL\sigma_T}$

- Normalized magn. field:

$\boldsymbol{b = B/B_Q}$

$B_Q = m_e^2\, c^3/e\, h \approx 4.4\times10^{13}$ G

Qualitative Broadband Spectrum

$\overline{\gamma}^2 \sim 1/\tau_T$

- Two small dimensionless parameters:
  - Thomson optical depth, $\boldsymbol{\tau_T = nL\sigma_T}$
  - Normalized magnetic field $\boldsymbol{b = B/B_Q}$, $B_Q = m_e^2\, c^3/e\, h \approx 4.4\times10^{13}$ G
- Characteristic synchrotron photon energy:

$\varepsilon_{sync} \sim \gamma^2\, h\nu_c \sim \tau_T^{-1}\, h\nu_c \sim \tau_T^{-1}\, b\, m_e c^2$, where $\nu_c = eB/2\pi\, m_e c$ – cycl. frequency

- Characteristic SSC photon energy:

$\varepsilon_{SSC} \sim \gamma^2\, \varepsilon_{sync} \sim \tau_T^{-1}\, \varepsilon_{sync} \sim \tau_T^{-2}\, h\nu_c \sim \tau_T^{-2}\, b\, m_e c^2$

- Higher order inverse-Compton (IC) components:

$\varepsilon_n \sim \gamma^2\, \varepsilon_{n-1} \sim \tau_T^{-1}\, \varepsilon_{n-1} \sim \tau_T^{-2}\, \varepsilon_{n-2} \sim \ldots \sim \tau_T^{-n}\, \varepsilon_0 \sim \tau_T^{-(n+1)}\, b\, m_e c^2$

(n=0 – synch., n=1 – SSC, etc.)

- Max. number *N* of IC components is limited by Klein-Nishina:

$\varepsilon_n \sim \tau_T^{-(N+1)}\, b\, \cancel{m_e} c^2 \sim \gamma\, \cancel{m_e} c^2 \;\Rightarrow$ $\boldsymbol{N \approx (\ln b)/(\ln \tau_T) - 1/2}$

SUMMARY 2

- Thermal balance between turbulent heating and synchrotron (+SSC) cooling --- both $\sim B^2/8\pi$ --- yields a statistical steady state with temperature

$$\boldsymbol{\theta = T/m_e c^2 \sim \tau_T^{-1/2}} \quad (\text{where } \tau_T = n_e L \sigma_T \ll 1)$$

- Synchrotron-Self-Compton (SSC) cooling (and perhaps a few higher-order inverse-Compton components) is automatically comparable to synchrotron cooling.

- Broadband spectrum – several roughly comparable peaks separated by a factor of τ_T^{-1} in photon energy.

3. Theoretical Model of Relativistic NTPA in Magnetic Reconnection

- Key Ingredients:
  - Acceleration by reconnection electric field E_{rec};
  - Magnetization by reconnected magnetic field B_y: *power-law slope*
  - Trapping in plasmoids: *high-energy cutoff*

Physical Picture: Reconnection

- Plasmoid-dominated magnetic reconnection plasmoid chain, characterized by a plasmoid distribution function $F(w)$ and a cumulative distribution $N(w)$:

$$N(w) = \int_{w}^{w_{\max}} F(w')dw'$$

- Reconnection may or may not be relativistic.
- Reconnection rate: $E_{rec} = \beta_{rec} B_0 = \varepsilon V_A B_0/c = \varepsilon \beta_A B_0$

$$V_A = c\beta_A = c\frac{\sqrt{\sigma_h}}{\sqrt{1+\sigma_h}}$$

  – "Hot" magnetization: $\boldsymbol{\sigma_h = B_0^2/(4\pi\, nh)}$; h = relativistic enthalpy.

  rel. limit: $\boldsymbol{\sigma}_h \gg 1 \rightarrow V_A \sim c$

  non-rel. limit $\boldsymbol{\sigma}_h \ll 1 \rightarrow \beta_A = V_A/c \sim \boldsymbol{\sigma}_h^{1/2} \ll 1$.

  – Cold $\boldsymbol{\sigma = B_0^2/(4\pi\, n_b\, mc^2)}$

- But particles under consideration are ultra-relativistic.

Self-similar hierarchical plasmoid chain

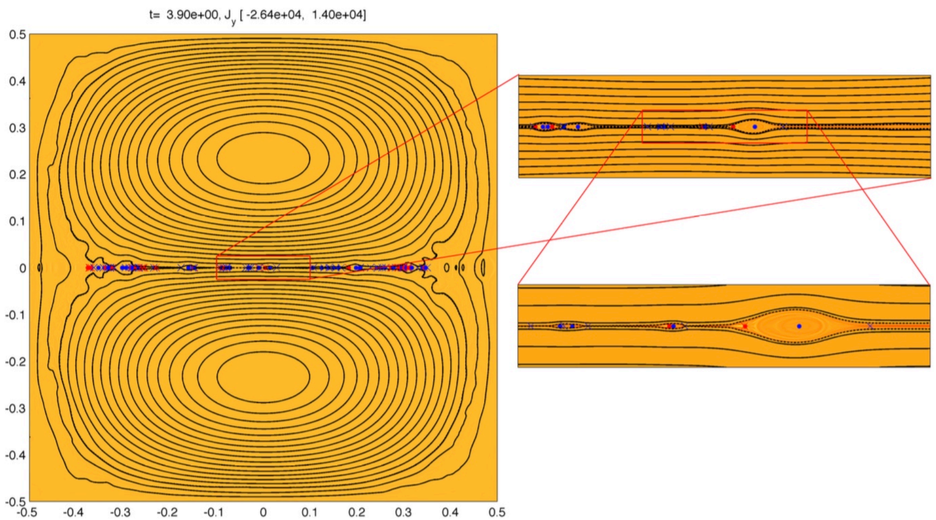

Bhattacharjee et al. 2009

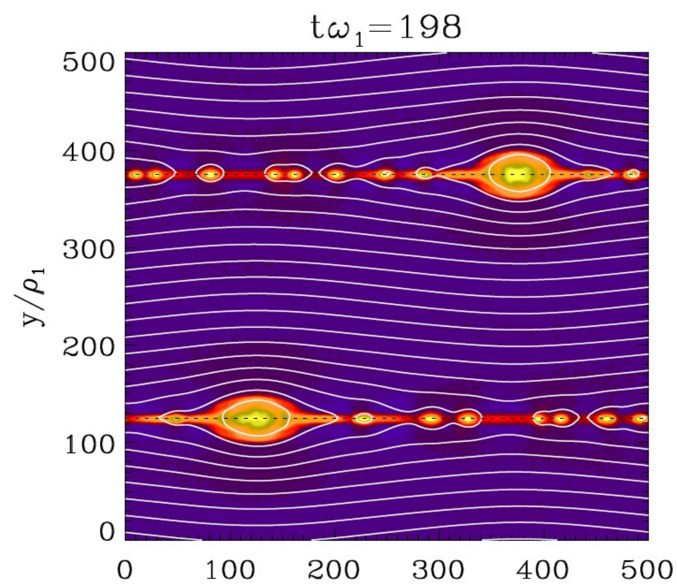

Cerutti et al. 2013

Two Phases of Reconnected Magnetic Field:

- of order $B_1 = \varepsilon B_0 = 0.1\ B_0$ in current sheets
- of order B_0 in plasmoids

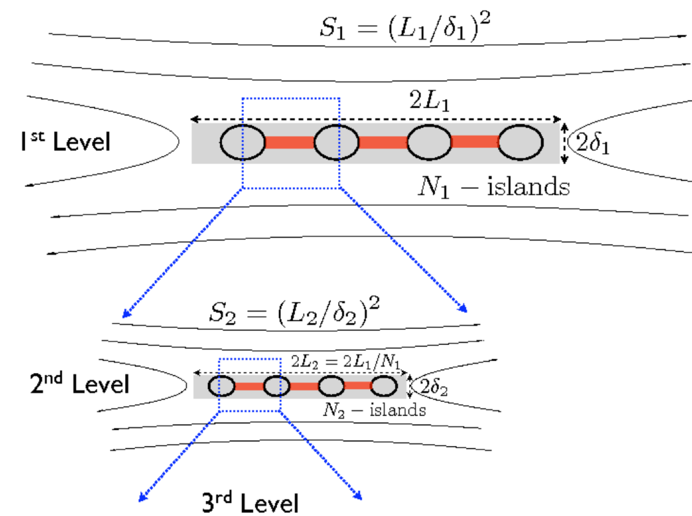

Empirical Numerical Properties of Reconnection-driven relativistic NTPA

Power-law index *p*

- *p* scales with $\boldsymbol{\sigma_h}$ as

$$p \sim C_1 + C_2 / \boldsymbol{\sigma_h}^{1/2}$$

p(σ)

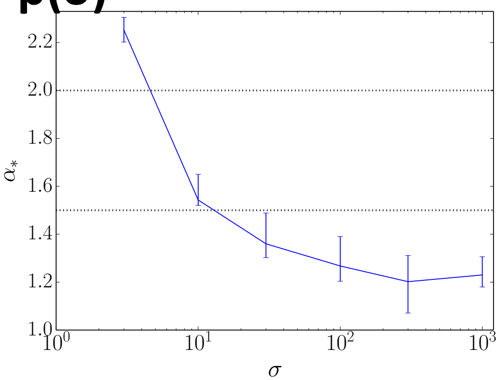

pair plasma:
Werner et al. 2016

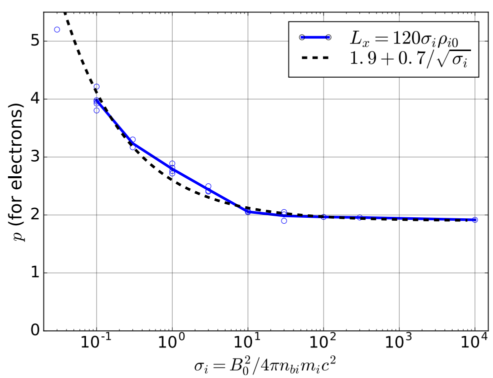

electron-ion plasma:
Werner et al. 2018

High-energy cutoff

(Werner et al. 2016)

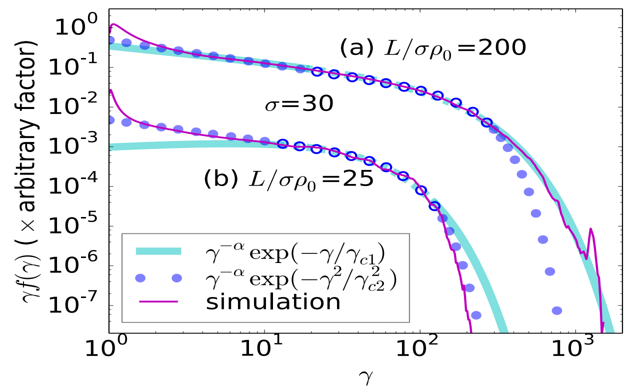

$$f(\gamma) = \frac{dN}{d\gamma} \propto \gamma^{-\alpha} \exp\left(-\gamma/\gamma_{c1} - \gamma^2/\gamma_{c2}^2\right)$$

Two high-energy cutoffs:

- $\exp(-\gamma/\gamma_{c1})$; $\boldsymbol{\gamma_{c1} \sim 4\sigma}$,
- $\exp[-(\gamma/\gamma_{c2})^2]$; $\boldsymbol{\gamma_{c2} \sim 0.1\, L/\rho_0}$

($\rho_0 = m_e c^2/e B_0$)

(guide magnetic field suppresses NTPA, see below)

Why is there a $\gamma_c \approx 4\sigma$ cutoff?

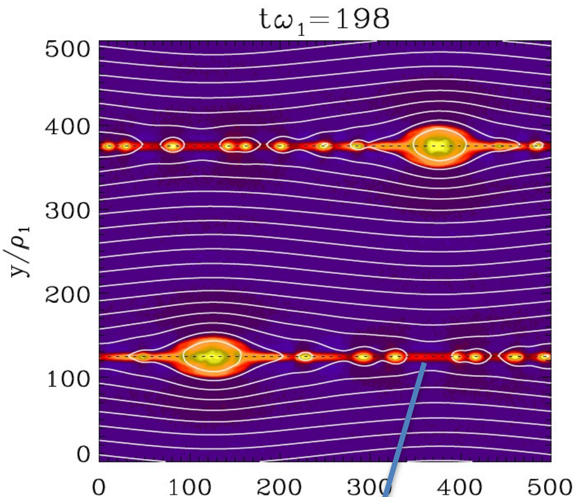

Cerutti et al. 2013

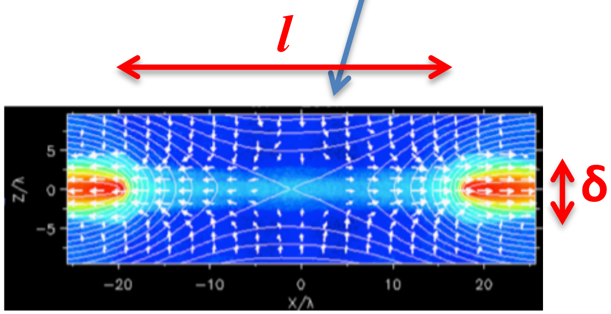

Zenitani & Hoshino 2001

($\rho_0 = m_e c^2/e B_0$)

$\sigma = B_0^2/(4\pi\, nmc^2)$

- Cutoff comes from small laminar ***elementary inter-plasmoid layers*** at the bottom of the plasmoid hierarchy (marginally stable to tearing).
- Particles are accelerated in these layers but then become **trapped inside plasmoids**.

- Cutoff: $\boldsymbol{\gamma_c} = e E_{rec}\, l / m_e c^2 \approx 0.1\, e B_0\, l / m_e c^2 = \mathbf{0.1}\, \boldsymbol{l/\rho_0}$.
- Layers are marginally stable to tearing → $\boldsymbol{l \sim 100\, \delta}$.
- Layer thickness: $\boldsymbol{\delta} \approx \rho(\langle\gamma\rangle) = \langle\gamma\rangle \rho_0 \approx \boldsymbol{(\sigma/3)\, \rho_0}$.
- Thus, $\boldsymbol{l/\rho_0 \approx 100\, \delta/\rho_0 \approx 30\, \sigma}$ **=>** $\boldsymbol{\gamma_0 = 3\,\sigma}$.

Further particle acceleration is possible, e.g., in plasmoid mergers, but this 2nd-stage reconnection acceleration occurs with lower sigma and smaller *L*.

Kinetic Equation

$$\partial_t f(\gamma, t) = -\partial_\gamma(\dot{\gamma}_{\rm acc} f) - \frac{f(\gamma)}{\tau_{\rm magn}(\gamma)} - \frac{f(\gamma)}{\tau_{\rm tr}(\gamma)}$$

Key Ingredients:

- Acceleration by main reconnection electric field:

$$\dot{\gamma}_{\rm acc} = eE_{\rm rec}c/m_e c^2 = \epsilon\beta_A\Omega_0$$

- independent of γ …

- Magnetization by reconnected B-field (--> power-law):

$$\tau_{\rm mag}(\gamma) \sim \ell_{\rm mag}/c \sim \epsilon^{-1}\gamma\Omega_0^{-1}$$

- Trapping by large [w > $\rho_L(\gamma)$] plasmoids (→ cutoff):

  τ_{tr} controlled by plasmoid distribution function (below)

Steady-State Kinetic Equation

- Since $\dot{\gamma}_{acc}$ is independent of γ, we get

$$\dot{\gamma}_{\mathrm{acc}} \frac{\mathrm{d}f}{\mathrm{d}\gamma} = -\frac{f(\gamma)}{\tau(\gamma)}$$

- Solution:

$$f(\gamma) = C \exp\left(-\frac{1}{\dot{\gamma}_{\mathrm{acc}}} \int \frac{\mathrm{d}\gamma}{\tau(\gamma)}\right)$$

where

$$\frac{1}{\tau(\gamma)} = \frac{1}{\tau_{\mathrm{magn}}(\gamma)} + \frac{1}{\tau_{\mathrm{trap}}(\gamma)}$$

Magnetization by Reconnected Field and NTPA power law

- Energetic particle passes right through small plasmoids.
- Distance a particle travels before being magnetized

  $l_{mag}(\gamma) \sim \rho_L(\gamma, B_1) = (B_0/B_1)\, \rho_L(\gamma, B_0) = \varepsilon^{-1} \rho_0\, \gamma$
- magnetization time-scale $\tau_{\rm mag}(\gamma) \sim \ell_{\rm mag}/c \sim \epsilon^{-1}\gamma\Omega_0^{-1}$

- Balance magnetization with acceleration in kinetic eqn:
- power-law solution $f(\gamma) \sim \gamma^{-p}$
- **power-law index:** $p = p(\sigma_h) \sim \frac{1}{\beta_A} = \sqrt{\frac{1+\sigma_h}{\sigma_h}}$
  - ultra-rel (σ_h>>1): p → const (cf. Zenitani & Hoshino 2001)
  - non-rel. case (σ_h>>1): $p \sim \sigma_h^{-1/2}$ (c.f., Werner et al. 2018)

Plasmoid Chain I: single power-law

- Energetic particles can be trapped in "*large*" plasmoids when $w = w(\gamma) \sim \rho_L(\gamma) = \rho_0\,\gamma$ $\quad (\rho_0 = m_e c^2/e B_0)$
- **High-energy cutoff** is controlled by plasmoid distribution function $F(w) = -\,dN/dw$.
- $\tau_{\,trap} \sim \lambda_{pl}(w)/c$

where $\lambda_{pl}(w)$ is separation between plasmoids of size w:

- $\lambda_{pl}(w) = L/N(w)$
- Thus, $\tau_{trap}(\gamma) \sim L/cN(w{=}\gamma\rho_0)$

Single-Power-law plasmoid chain

- Consider for illustration: $F(w) \sim w^{-\alpha}$ for $w < w_{max}$
- Cumulative distribution: $N(w) \sim (w/w_{max})^{1-\alpha}$

[where $N(w_{max}) = 1$]

$$\tau_{\rm trap}^{-1}(\gamma) \sim \frac{c}{L} N[w(\gamma)] \sim \frac{c}{L} \left(\frac{\gamma}{\gamma_{\rm max}}\right)^{1-\alpha}, \quad \alpha \neq 1$$

where $\gamma_{max} = w_{max}/\rho_0$

- Special case $\alpha = 2$: $\tau_{trap} \sim \gamma$ (same as for magnetization - later)
- Trapping rate overtakes magnetization at

$$\gamma_c = \gamma_{\rm max} \left(\frac{w_{\rm max}}{\epsilon L}\right)^{\frac{1}{\alpha-2}}.$$

- For $w_{max} \sim \varepsilon L$: $\gamma_c \sim \gamma_{max}$

Establishing Cutoff

- Balancing acceleration against trapping in plasmoids:

$$f(\gamma) \sim \exp\left[-\frac{w_{\max}}{\epsilon\beta_A L(2-\alpha)}\left(\frac{\gamma}{\gamma_{\max}}\right)^{2-\alpha}\right]$$

- Special case $\alpha \sim 1$ (ignoring log-corrections)

$$f(\gamma) \sim \exp\left[-\frac{\rho_0}{L}\frac{1}{\beta_A\epsilon}\gamma\right] = \exp(-\gamma/\gamma_{c1})$$

- where $\gamma_{c1} \equiv \beta_A\epsilon\,\frac{L}{\rho_0} \simeq \beta_A\,\frac{w_{\max}}{\rho_0}$ (can be $< \gamma_{max}$, if $\beta_A < 1$)

- Special case $\alpha=2$: no cutoff but another power-law: $p \simeq \frac{1}{\epsilon\beta_A}\frac{w_{\max}}{L}$
  - For $w_{max} \sim \varepsilon L$: $p \sim \beta_A^{-1}$ (~same as without plasmoids)
  - Combined with magnetization: → steeper (by x2) power law.

Plasmoid Chain II: Realistic double-power-law

- Real simulations show double-power-law plasmoid distributions (Loureiro et al. 2012, Huang et al. 2013, Sironi et al. 2016, Petropoulou et al. 2018)

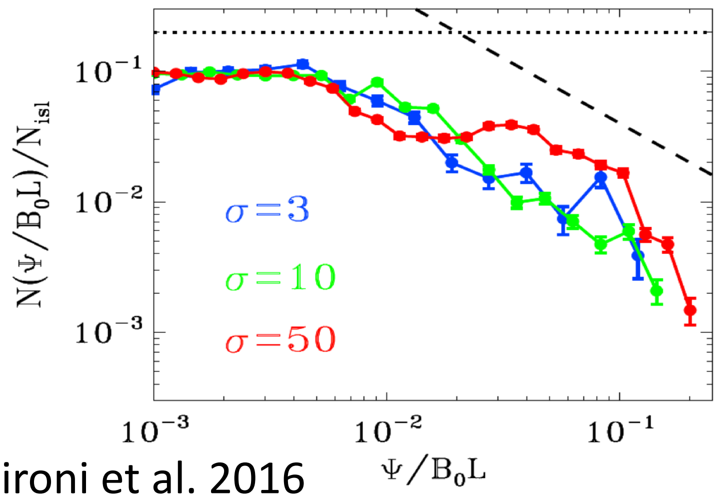

Sironi et al. 2016

$$F \sim w^{-\alpha_1}, \quad w < w_c$$

$$F \sim w^{-\alpha_2}, \quad w_c < w < w_{\max}$$

$$N(w < w_c) = N_c \left(\frac{w}{w_c}\right)^{1-\alpha_1}$$

$$N(w > w_c) = \left(\frac{w}{w_{\max}}\right)^{1-\alpha_2}$$

Most likely: $\alpha_1 \approx 1$, $\alpha_2 \approx 2$

$$\gamma_{\rm cutoff} = \gamma_c \left(\frac{w_c}{\epsilon \lambda_c}\right)^{\frac{1}{\alpha_1 - 2}} \sim \gamma_c = w_c/\rho_0$$

For $\alpha_1 \approx 1$: $\gamma_{\rm cutoff} = \gamma_c \left(\frac{\epsilon\lambda_c}{w_c}\right) \sim \gamma_c$

Important Question:

What controls w_c?

If $\alpha_2 \approx 2$: possible 2nd (steeper) power law above spectral break at γ_c

Important Question:

What controls w_c?

- Consider large-system regime: $L >> \delta \sim \langle\rho\rangle \sim \sigma \rho_0$
- The plasmoid distribution break size w_c may be anywhere between microscopic $\sim \sigma \rho_0$ and macroscopic $\sim L$.
- If $w_c \sim \sigma \rho_0$, then $\gamma_c \sim \sigma$, e.g., $\gamma_c \approx 4\sigma$ (Werner et al. 2016)
- If $w_c \sim L$, then $\gamma_c \sim L/\rho_0$ -- "extreme" (Hillas) acceleration limit.

Conclusions

Relativistic Nonthermal Particle Acceleration (NTPA) in reconnection is an interplay of:

– steady acceleration by reconnection electric field;

checked by "escape" from acceleration zone:

- (1) magnetization by general reconnected magnetic field $B_1 \sim 0.1\, B_0 \rightarrow$ power-law index

$$p \sim (E_{rec}/B_1)^{-1} \sim 1/\, \beta_A \sim [1+\sigma_h)/\sigma_h]^{1/2}$$

- (2) capture/trapping by plasmoids with $w \sim \rho_L(\gamma) = \gamma\, \rho_0$. $\rightarrow$ high-energy cutoff.
- Cutoff depends on plasmoid-distribution function, e.g., for α=1 it is simple exponential with $\gamma_c = w_{max}/\rho_0$.
- Realistic double-power-law F(w): cutoff at break size w_c and
- possible steeper power law (if $\alpha_2 \approx 2$) above w_c